EUROPEAN FUSION DEVELOPMENT AGREEMENT

EFDA–JET–PR(04)59

P.U. Lamalle, M.J. Mantsinen, J.-M. Noterdaeme, B. Alper, P. Beaumont, L. Bertalot, T. Blackman, V.V. Bobkov, G. Bonheure, J. Brzozowski, C. Castaldo, S. Conroy, M. de Baar, E. de la Luna, P. de Vries, F. Durodié, G. Ericsson, L.-G. Eriksson, C. Gowers, R. Felton, J. Heikkinen, T. Hellsten, V. Kiptily, K. Lawson, M. Laxåback, E. Lerche, P. Lomas, A. Lyssoivan, M.-L. Mayoral, F. Meo, M. Mironov, I. Monakhov, I. Nunes, G. Piazza, S. Popovichev, A. Salmi, M.I.K. Santala, S. Sharapov, T. Tala, M. Tardocchi, D. Van Eester, B. Weyssow and JET EFDA contributors

Expanding the Operating Space of ICRF on JET with a view to ITER

Expanding the Operating Space of ICRF on JET with a view to ITER

P.U. Lamalle[1a], M.J. Mantsinen[2a], J.-M. Noterdaeme[3,14], B. Alper[4], P. Beaumont[4], L. Bertalot[5a], T. Blackman[4], V.V. Bobkov[3], G. Bonheure[1a], J. Brzozowski[8], C. Castaldo[5a], S. Conroy[8], M. de Baar[9], E. de la Luna[6], P. de Vries[4], F. Durodié[1a], G. Ericsson[8b], L.-G. Eriksson[7], C. Gowers[4], R. Felton[4], J. Heikkinen[2b], T. Hellsten[8a], V. Kiptily[4], K. Lawson[4], M. Laxåback[8a], E. Lerche[1a], P. Lomas[4], A. Lyssoivan[1a], M.-L. Mayoral[4], F. Meo[10], M. Mironov[11], I. Monakhov[4], I. Nunes[12], G. Piazza[13], S. Popovichev[4], A. Salmi[2a], M.I.K. Santala[2a], S. Sharapov[4], T. Tala[8a], M. Tardocchi[5b], D. Van Eester[1a], B. Weyssow[1b] and JET EFDA contributors*

[1]Association EURATOM - Belgian State[+], Brussels, Belgium: [a]Plasma Physics Laboratory, Royal Military Academy, 30 av. de la Renaissance; [b]PTM-ULB.
[2]Association EURATOM-Tekes, [a]HUT / [b]VTT, Helsinki, Finland.
[3]Max-Planck IPP-EURATOM Assoziation, Garching, Germany.
[4]EURATOM/UKAEA Fusion Association, Culham Science Centre, Abingdon, U.K.
[5]Associazione EURATOM-ENEA sulla Fusione, [a]Frascati / [b]CNR Milano, Italy.
[6]Asociación EURATOM-CIEMAT, Laboratorio Nacional de Fusion, Spain.
[7]Association EURATOM-CEA, CEA-Cadarache, France.
[8]Association VR-EURATOM, Sweden: [a]Alfvén Laboratory; [b]Uppsala University.
[9]FOM-Rijnhuizen, Association EURATOM-FOM[+], Nieuwegein, The Netherlands.
[10]Risø, Association EURATOM-Denmark, Kopenhagen, Denmark.
[11]Ioffe Physico-Technical Institute, St Petersburg, Russia.
[12]Associação EURATOM-IST, Instituto Superior Técnico, Portugal.
[13]Forschungszentrum Karlsruhe, IKET, Germany.
[14]Gent University, EESA, Belgium. [+]Partners in the Trilateral Euregio Cluster (TEC).
** See annex of J. Pamela et al, "Overview of Recent JET Results and Future Perspectives", Fusion Energy 2002 (Proc.19 [th] IAEA Fusion Energy Conference, Lyon (2002).*

Preprint of Paper to be submitted for publication in
Nuclear Fusion

ABSTRACT

The paper reports on ITER-relevant ICRF physics investigated on JET in 2003 and early 2004: minority heating of ^{3}He and D in H plasmas, minority heating of tritium in D, investigations of finite Larmor radius effects on the RF-induced high-energy tails, fast wave heating and current drive, and new results on the heating efficiency of ICRF antennas. ELM studies using fast RF measurements, experimental demonstration of a new ELM-tolerant antenna matching scheme, and technical enhancements planned on the JET ICRF system for 2005, themselves likewise strongly driven by the preparation for ITER, are also summarized.

1. INTRODUCTION

The size and capability of the Joint European Torus (JET) to confine very energetic particles, together with its versatile Ion Cyclotron Resonance Frequency (ICRF) system, provide a unique environment to develop ICRF techniques relevant to the Next Step. During the JET experimental campaigns of 2003 and early 2004, in addition to further development of ICRF as a tool for the experimental programme, several heating and current drive scenarios have been investigated, contributing to the physics understanding and operational expertise required for successful use of ICRF on ITER. The following sections focus on these advances. Three hitherto scarcely documented 'inverted' minority heating scenarios, in which the minority ions have a smaller charge to mass ratio than the majority ones, have received special attention: ICRF heating of helium three (^{3}He) and deuterium (D) in hydrogen (H) plasmas, which are the scenarios planned for the start-up phase of ITER, and minority heating of tritium (T), which would be an attractive scenario when ITER starts using T. Investigations of finite Larmor radius effects on the RF-induced high-energy tails are summarized in Section 4, fast wave heating and current drive experiments in Section 5 and new results on the heating efficiency of ICRF antenna arrays in Section 6. The remainder of the paper reports on topics of a more technical nature: studies of the ELMs using fast RF measurements, experimental demonstration of a new ELM-tolerant antenna matching scheme, and the technical enhancements planned on the JET ICRF system, themselves likewise strongly driven by the preparation for ITER.

2. ICRF HEATING IN HYDROGEN PLASMAS

In the start-up phase of ITER, activation will at first be minimized by operating in H plasmas. The two reference ICRF scenarios, known as (^{3}He)H and (D)H, rely on heating minority ^{3}He or D ions at their fundamental cyclotron frequency. In the past very few experiments have been dedicated to these scenarios [1] in which an ion-ion hybrid resonance/cut-off pair of the fast magnetosonic wave occur on the antenna side of the minority cyclotron layer. The heating of ^{3}He in H has now been explored in a sequence of JET discharges at magnetic fields between 3.3 and 3.6T and a plasma current of 2MA. The ICRF power was applied at 37MHz, which positions the cyclotron resonance layer $\omega=\omega_{c^3He}$ centrally. The experiments systematically used ICRF power modulation at a frequency of 20Hz at the beginning and the end of the power flat-top (see Fig.1), allowing evaluation of the radial profiles of wave absorption by the electrons by means of Fast Fourier Transform (FFT) and

break-in-slope (BIS) analysis [2,3] of the electron temperature response. The ^{3}He concentration [^{3}He] = $n_{^3He}/n_e$ was varied from below 1% up to 10%. The expertise developed at JET to estimate and control [^{3}He] in real time [3] was put to full use and levels as low as 1.8% were successfully controlled for the first time. Lower [^{3}He] were obtained by ^{3}He gas puffing before the ICRF heating phase.

The minority heating (MH) regime was observed at low concentrations (up to ~2%). Presence of a fast ^{3}He ion population was detected by *(i)* its contribution to the neutron rate through the nuclear reaction ^{9}Be(^{3}He,n)^{11}C; *(ii)* gamma-ray spectrometry [4] based on nuclear reactions between energetic ^{3}He, ^{9}Be and ^{12}C impurities, and *(iii)* low- and high-energy neutral particle analysis (NPA) [5]. Figure 1 shows three discharges with [^{3}He]<1% and 5MW of ICRF in different A2 antenna phasings [6]: dipole ($0\pi0\pi$) launches waves with a symmetric toroidal spectrum; +90º and −90º progressive phasings launch dominantly co- and counter-current waves, respectively. A maximum electron temperature of 6.2keV was reached with +90º. Higher neutron rate, fast ^{3}He energy content, NPA flux and g-ray emissivity are obtained with +90º than with matching discharges in the other phasings. Such behaviour can be explained in terms of an inward fast ion orbit pinch produced by the +90º wave spectrum [7, 8], for which multiple evidence has previously been accumulated in phased ICRF experiments on JET.

As [^{3}He] was increased above 2%, a sudden transition was reproducibly observed to the Mode Conversion (MC) regime, in which the ICRF fast wave couples to a short wavelength mode, leading to efficient direct electron heating. The first indication of a change in the heating regime was the disappearance of the fast ^{3}He population. The related changes in γ-ray emission, for which the threshold ^{3}He energy is 0.9MeV, are shown on Fig.2 for three discharges differing only by their [^{3}He]. In Pulse No: 63319 with [^{3}He] <1.8% a high signal was collected throughout. In Pulse No: 63320, as [^{3}He] increased above 2% at ≈6.3s, the γ-ray signal began to decrease and finally disappeared. In Pulse No: 63324, almost no signal was collected. Moreover, as [^{3}He] increased, the temperature response to the ICRF power modulation gradually changed, indicating a change in power deposition. In the MH regime, electron heating takes place indirectly by collisions with fast ions and the period of the ICRF power modulation (0.05s) associated with an estimated fast ^{3}He slowing-down time of about 0.2s prevented observation of a clearcut T_e response. In contrast, electron heating in the MC regime takes place directly by wave Landau damping and a prompter T_e response was observed. The transition to the MC regime was also confirmed by the FFT and BIS analyses which showed the apperance of a narrow electron power deposition profile at the estimated location of the ion-ion hybrid layer. Figure 3 presents an overview of two discharges in the MC regime ([^{3}He] ~3.5%) with dipole and +90º phasing. In order to maximize the central T_e, the toroidal field was lowered to 3.3T, positioning the ion-ion hybrid layer at around 2.8m. A maximum temperature of 8keV was obtained with dipole phasing. A comparative code analysis of the two pulses is under way to confirm the difference in dominant $k_{//}$ as the origin of the higher temperature obtained in dipole.

In strong contrast with ^{3}He, the use of D minority heating in hydrogen plasmas was not successful. This is attributed to the C^{6+} impurity (and contributions from any other impurity with Z/A=1/2),

which has the same cyclotron layer as D and influences wave propagation like a sixfold as high number concentration of D. Presence of carbon at levels of 1 to 2% directly leads into the mode conversion regime or even expels the mode conversion layer from the plasma. This effect virtually rules out the (D)H scenario, leaving (^{3}He)H as the only viable scenario for the non-active phase of ITER.

3. MINORITY HEATING OF TRITIUM

Plasmas with low tritium concentration will occur when ITER starts using T. ICRF minority heating of T at its fundamental cyclotron frequency ($\omega=\omega_{cT}$) is a physically attractive though technically challenging heating scenario. On JET it requires the highest equilibrium magnetic fields (B_0=3.9 to 4T) and the lowest available generator frequency (~23MHz), at which only modest levels of ICRF power ~1.5MW are available. Although currently outside the ITER RF system frequency range, it would be quite relevant during its operation at low to moderate T concentrations. It was first very briefly investigated during the JET DTE1 experimental campaign of 1997 [9, 10] with ~5% T and on TFTR [9] with up to 20% T.

It has now been intensively studied at low concentrations in D plasmas during the Trace Tritium Experimental (TTE) campaign [11,12,13], in which T was introduced in the discharge by gas puffs resulting in concentrations up to ~3% (in a few discharges neutral beam T injection was used instead). Energetic T tails of 80 to 120keV were observed, close to the maximum of the D-T reaction rate, boosting the D-T neutron yield by direct T acceleration, and simultaneously providing good bulk electron heating (Fig.4). The moderate triton tail energies also provide good ion heating (off-axis in the JET configuration). This confirms the scenario as an attractive heating scheme at low concentration. Its possible incorporation in the ITER ICRF design should be revisited after further experiments at intermediate T concentrations, e.g. during a full D-T campaign on JET. Detailed interpretation and modelling of the ICRF in TTE benefit from the neutron and gamma ray emissivity data, which allow interesting code benchmarks and enhancements. Figure 5 shows the good agreement found between the high-field-side (HFS) peaking of the 2D neutron emissivity profile and the corresponding fast triton midplane density simulated with the SELFO code [14], which also correctly estimates the experimental neutron yield and T tail temperature.

4. FINITE LARMOR RADIUS (FLR) EFFECTS ON THE ICRH MINORITY ION TAILS

Wave absorption at the second ion cyclotron harmonic ($\omega=2\omega_c$) depends on the ratio of the particle Larmor radius to the wavelength $\lambda_\perp$. Theory predicts a maximum absorption when this ratio increases to ~ 0.5, followed by a decrease to much smaller levels at higher ratios. This behaviour defines a characteristic particle energy E^* at which the RF quasilinear diffusion coefficient has a first minimum. This absorption-free region acts as a barrier preventing particles from reaching higher energies. At fixed magnetic field, $E^* \propto \lambda_\perp^{\,2}$ is inversely proportional to the density. Minority hydrogen ions were heated at their second cyclotron harmonic $2\omega_{cH}$ with 3 to 5MW of ICRF (51MHz, dipole phasing) in 1.65T, 1.65MA JET deuterium discharges with central electron densities between 3 and $4\text{x}10^{19}$ m^{-3} (i.e. different wavelengths). Fast hydrogen energy distributions were measured with a

high-energy Neutral Particle Analyzer (NPA) [15]. Fig. 6 shows that, at similar heating powers per particle and Stix effective H tail temperatures Teff, a higher plasma density yields a less energetic H tail with a lower local temperature. This provides clear evidence that FLR effects play an important role in determining the shape of the high energy part of the distribution. FIDO [16] code simulations are in good agreement with these measurements [17]. Note that this type of experiment requires confining protons in the MeV range and can thus only be performed on JET.

5. FAST WAVE HEATING AND CURRENT DRIVE (FWHCD) EXPERIMENTS

FWHCD has been studied in JET internal transport barrier plasmas at B_0=3.4T and RF power up to 6MW at f=37MHz (the same f/B_0 as planned for ITER). A comprehensive account of the experiments can be found in [18]. Traces of residual ^{3}He absorbed significant RF power, reducing the fraction available for FWHCD via electron Landau damping and TTMP (on ITER similar power diversion is expected from T absorption at $2\omega_{cT}$). Despite low wave single pass damping (a few %), effective direct electron heating was observed in 0π0π. In ±90° only small changes of central current density were observed. This is attributed to the competition of parasitic ion absorption, the long current penetration time, and a large parasitic dissipation associated with RF sheaths, discussed in Section 6. On ITER the latter loss channel should be less of a problem for current drive, assuming careful antenna design. However the $2\omega_{cT}$ tritium absorption will be difficult to avoid, and the characteristic time for changing the current will be even longer than on JET.

6. NEW INVESTIGATIONS OF THE ICRF HEATING EFFICIENCY

In specific operating conditions substantial discrepancies are found between the power P_C launched by the A2 ICRF antennas and the plasma power balance. The power not accounted for in the bulk plasma is neither detected in the measured radiation nor in divertor heat loss. A 'core heating efficiency''η can be defined accordingly as $\eta = \mathbf{P_{abs}} / \mathbf{P_C}$, where P_{abs} is the ICRF bulk power absorption. η can be estimated in relative terms by comparing discharges, and in absolute terms by power balance analysis and comparisons with code simulations including the relevant wave collisionless damping mechanisms.

L-mode discharges at B_T=2.7T, I_p=2 and 2.8MA were compared to further investigate the behaviour of η [19]. ICRF power ramps up to 8MW in various antenna phasings using 42MHz (H)D minority heating confirmed earlier observations [20]: η is maximum and typically >90% in dipole (0π0π), but only about half as much in monopole (0000) despite the much higher antenna coupling resistance. Also η(0ππ0)~0.9 η(0π0π), and η(00ππ) was slightly above η(0000). Other experiments were carried out in which only part of each A2 array was fed. Interestingly, antennas with only one or two active in-phase straps had an η 50% higher than the standard 0000 with four active straps. Comparing 0π0π with 0000 in this heating scenario, η is higher at higher wave single pass absorption (0p0p).

In the FWHCD experiments reported in Section 5 [18], h(0p0p) was similar to that of hydrogen minority heating in +90°. The heating efficiencies for ±90° FWCD phasings were η(+90°)~0.6

$\eta(0\pi0\pi)$ and $\eta(-90°)$~0.5 $\eta(0\pi0\pi)$, with a difference attributed to ^{3}He pinch orbit effects. Higher unaccounted power in ±90° phasings was correlated with lower single pass wave damping.

All the experiments confirm a strong dependence of the heating efficiency η on the radiated parallel wavenumber spectrum; the observations are consistent with parasitic ICRF absorption by RF sheath voltage rectification [21], smaller unaccounted power being associated with the phasing producing the lowest rectified sheath potential. Assuming an antenna design minimizing sheath effects, the higher single pass absorption expected on ITER for 0000 might result in a reduction of parasitic sheath dissipation, hence in a better monopole heating efficiency than on JET.

7. COUPLING STUDIES DURING ELMS

The strong antenna loading perturbations associated with ELMs induce large transient power reflection in the RF transmission systems which severely limits the ICRF power delivered to ELMy H mode plasmas. ELM-resolved RF measurements on the antennas provide invaluable data to estimate the performance of future launchers [22]. Systematic observations of the perturbations of RF voltages associated with the rise of type I ELMs have shown that these perturbations propagate in the counter-current direction (the same direction as the electron diamagnetic drift), in agreement with the fast magnetic measurements. Typical toroidal velocities ~ 200km/s (generally between 50 and 1200km/s) are observed, corresponding to a toroidal period ~ 120μs. The highest velocities were seen in low density discharges. Therefore for most of the observed ELMs, the delays between antenna straps situated in the same toroidal octant should have marginal or negligible effect on the operation of the compensation networks of the ELM-resilient ICRF systems described in the next Sections.

8. ELM TOLERANT MATCHING PROOF OF PRINCIPLE

A prototype ELM-tolerant ICRF antenna matching system has been successfully tested at JET [23]. The technique is based on the same principle as proposed for ITER [24], but uses a matching circuit tuned to a low reference impedance by coaxial line stretchers outside the tokamak vacuum vessel, like the alternative ITER ICRF design option proposed in [25]. Further impedance transformation to the main power transmission line is achieved by a conventional variable stub and trombone tuner. The experimental setup involved one pair of adjacent straps of the A2 antenna array powered by a single RF amplifier. The tests fully confirm the feasibility of the matching scheme. Clear evidence of high load tolerance was observed during plasma sawtooth activity and ELMs, see Fig.7. Reliable trip-free performance was demonstrated from 32 to 51MHz. This approach appears a viable alternative to in-vessel matching schemes and offers additional advantages such as exclusive reliance on well-established coaxial line technology, manageable tuning accuracy requirements, separation of launching and matching sub-systems, and capability to conjugate remote antenna straps.

9. FORTHCOMING ENHANCEMENTS TO THE JET ICRF SYSTEM

A major JET enhancement is under way with the scheduled installation of an additional ITERlike ICRF antenna in 2005-2006 [26], shown on Fig. 8, which will be a key test of the ITER concept. It

aims at validating novel antenna design principles in conditions as relevant as possible to ITER by coupling ~7.2MW to ELMy H-mode plasmas between 30 and 55MHz. The high power density (≈8MW/m^2) is maximized by using poloidally short straps, and the resilience to fast varying RF loads by matching pairs of straps (in-vessel) in so-called conjugate-T circuits. This is accompanied by the addition of 3dB hybrid couplers in the transmission systems of two of the four existing A2 antennas, and a likely implementation of line stretcher conjugate T matching (see Section 8) on the remaining two antennas. Concurrent use of these enhancements will allow a unique comparison of their performance. They will provide additional power for a wide range of conditions, in particular at low frequency (minority heating of 3He, second harmonic heating of T, relevant to a future D-T campaign), and in presence of ELMs, further expanding the relevance of the JET ICRF system for ITER.

ACKNOWLEDGEMENTS

This work was conducted under the European Fusion Development Agreement. It is a pleasure to thank the staff who operated the JET tokamak, its heating systems and diagnostics. The work carried out by the UKAEA personnel was jointly funded by the United Kingdom Engineering and Physical Sciences Research Council and by EURATOM. The work of E.L. is supported by the EU under a EURATOM Intra-European Fellowship.

REFERENCES

[1]. V.B. BHATNAGAR, *et al.*, Proc. 25th EPS Conf. on Plasma Physics, Prague, Czech Republic (1998) 1178.
[2]. D.J. GAMBIER, *et al.*, Nucl. Fusion **30** (1990) 23-24.
[3]. D. VAN EESTER, *et al.*, in Radio Frequency Power in Plasmas, AIP Conf. Proceedings **694** (2004), Ed. C.B. Forest, Melville, New York.
[4]. V. KIPTILY *et al.*, Nucl. Fusion 42 (2002) 999.
[5]. A.A. KOROTKOV, A. GONDHALEKAR, A.J. STUART, Nucl. Fusion **37** (1997) 35.
[6]. A. KAYE, *et al.*, Fusion Engineering and Design **24** (1994) 1.
[7]. L. CHEN, J. VACLAVIK, G.W. HAMMETT, Nucl. Fusion (1988) **28** 389.
[8]. M.A.KOVANEN, CORE, W.G.F., HELLSTEN, T., Nucl. Fusion **32** (1992) 787.
[9]. The JET and TFTR TEAMS, presented by D Start, Plasma Phys. Control. Fusion **40** (1998) A87.
[10]. D.F.H. START, *et al.*, Nucl. Fusion **39** (1999) 321.
[11]. P.U. LAMALLE, M.J. MANTSINEN, *et al.*, Proc. 31st EPS Conf. on Plasma Physics, London, ECA **28G** (2004) P-5.165.
[12]. K-D. ZASTROW, *et al.*, Proc. 31st EPS Conf. on Plasma Physics, London, ECA **28G** (2004).
[13]. D. STORK, *et al.*, these Proceedings, paper OV/4-1.
[14]. J. HEDIN, *et al.*, Plasma Phys. Control. Fusion **40** (1998) 1085.
[15]. A.A. KOROTKOV, A. GONDALEKHAR, A.J. STUART, Nucl. Fusion **37** (1997) 35.
[16]. J. CARLSSON, L.-G. ERIKSSON, T. HELLSTEN, Nucl. Fusion **32** (1997) 719.
[17]. A. SALMI, *et al.*, to be submitted to Plasma Phys. Control. Fusion.

[18]. T. HELLSTEN, M. LAXÅBACK, *et al.*, to be submitted to Nuclear Fusion.
[19]. J. HEIKKINEN, *et al.*, Proc. 31st EPS Conf. on Plasma Physics, London, ECA **28G** (2004) P-5.162.
[20]. D.F.H. START, *et al.*, AIP Conf. Proceedings 355 (1995) 7.
[21]. D.A. D'IPPOLITO, J.R. MYRA, M. BURES, J. JACQUINOT, Plasma Phys. Control. Fusion **33** (1991) 607.
[22]. V.V. BOBKOV, *et al.*, Proc. 31st EPS Conf. on Plasma Physics, London, ECA **28G** (2004) P-1.141.
[23]. I. MONAKHOV, *et al.*, Proc. 23rd SOFT, Venice, 2004, to appear in Fusion Eng. & Design.
[24]. G. BOSIA, Fusion Science and Technology **43** (2003) 153.
[25]. A. MESSIAEN, *et al.*, in Radio Frequency Power in Plasmas, AIP Conf. Proceedings **694** (2004) 142, Ed. C.B. Forest, Melville, New York; DUMORTIER, P., et al., *ibid* p.94.
[26]. F. DURODIÉ, *et al.*, Proc. 23rd SOFT, Venice, 2004, to appear in Fusion Eng. and Design.

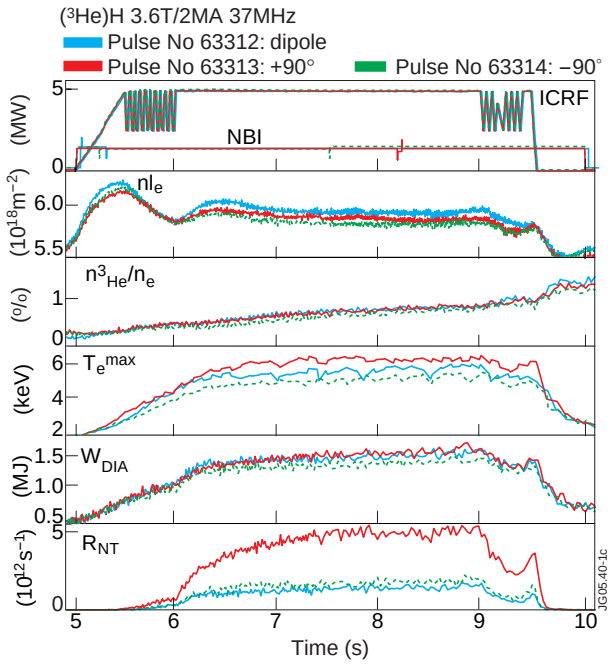

Figure 1: (^{3}He)H minority heating at [^{3}He]<1% with dipole, +90° and −90° antenna phasings (resp. blue, red, green). Note the much higher neutron yield R_{NT} achieved with +90°.

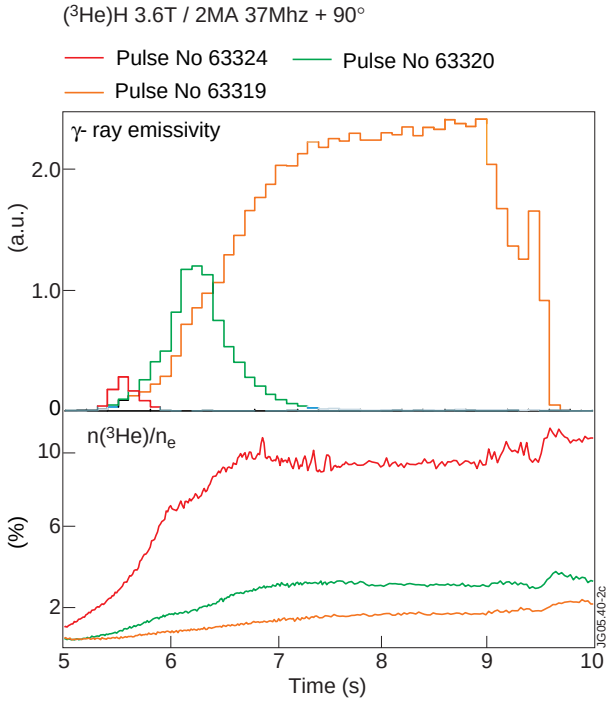

Figure 2: Time evolution of the γ-ray emissivity and ^{3}He concentration for three discharges, demonstrating disappearance of the fast ^{3}He population as [^{3}He] was increased above 2%.

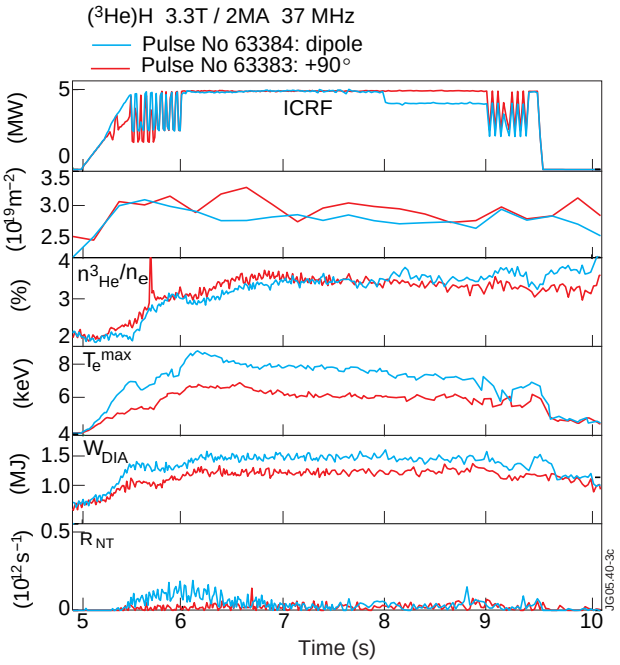

Figure 3: Mode conversion heating regime with 2<[^{3}He]<4%, dipole (blue) and +90° (red) phasings. The ion-ion hybrid layer is located at R≈2.8m.

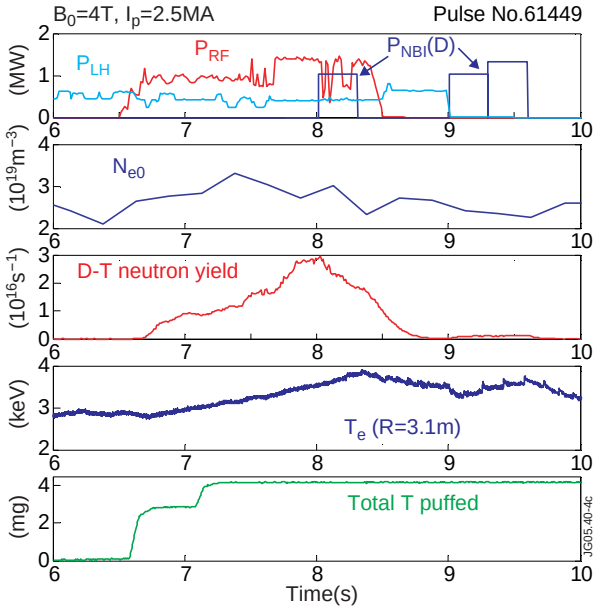

Figure 4: Fundamental ICRF heating of minority T introduced by gas puff (23MHz, 4T). Maximum neutron yield 2.9 10^{16}/s, maximum coupled RF power 1.4MW.

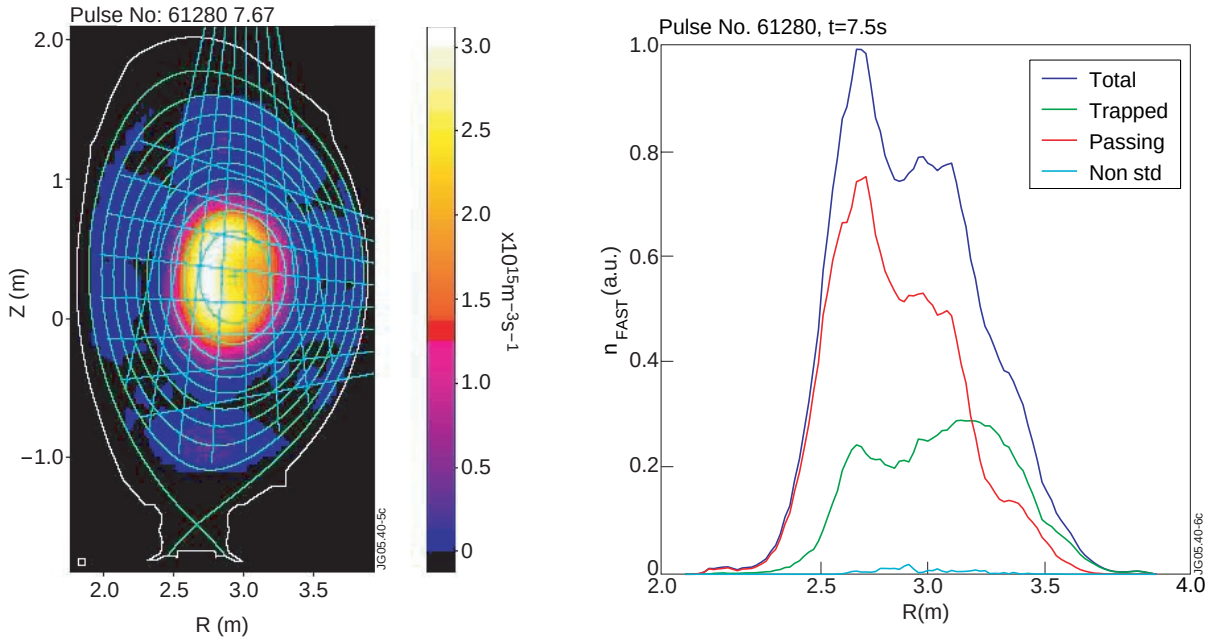

Figure 5: Left: D-T neutron emissivity profile at t=7.7s for (T)D ICRF heating (dipole phasing, 23MHz). Right: fast (E>50keV) triton midplane density simulated with the SELFO code for the same Pulse (No: 61280), showing contributions from passing, trapped and non standard orbits. The majority of D-T neutrons originate from passing tritons. Their higher density on the HFS of the magnetic axis is due to the longer time spent there, and is in good agreement with the observed neutron profile.

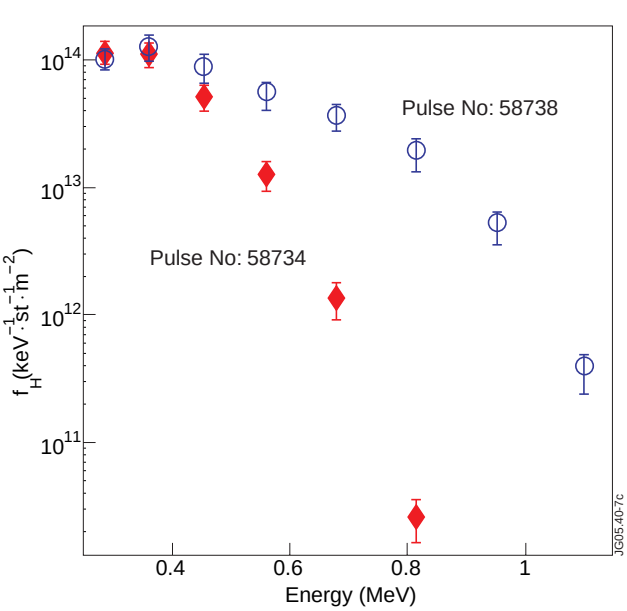

Figure 6: Perpendicular proton energy distributions measured with the NPA. Pulse No: 58734 and 58738 respectively have PRF=5 and 3MW, N_{e0}=4 and 3 x10^{19} m^{-3}, E ~ 1.03 and 1.37MeV, similar absorbed powers per particle and effective Stix tail temperatures.*

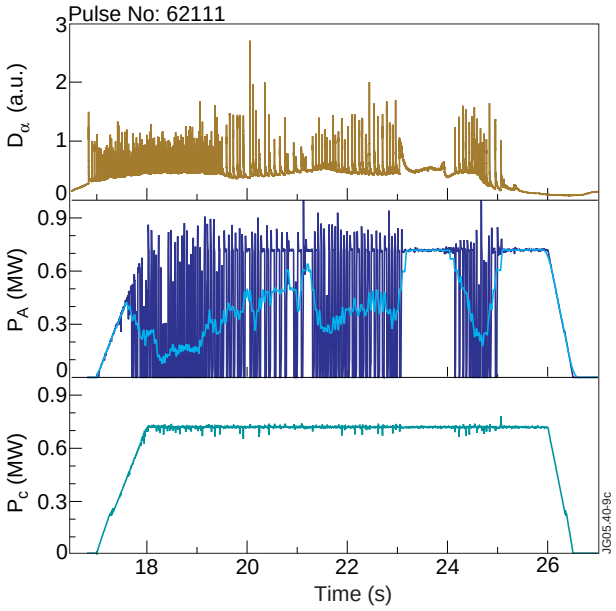

Figure 7: ICRF coupling to an ELMy plasma, showing powers P_A from standard A2 antenna and P_C from half antenna equipped with prototype load resilient external conjugate T system.

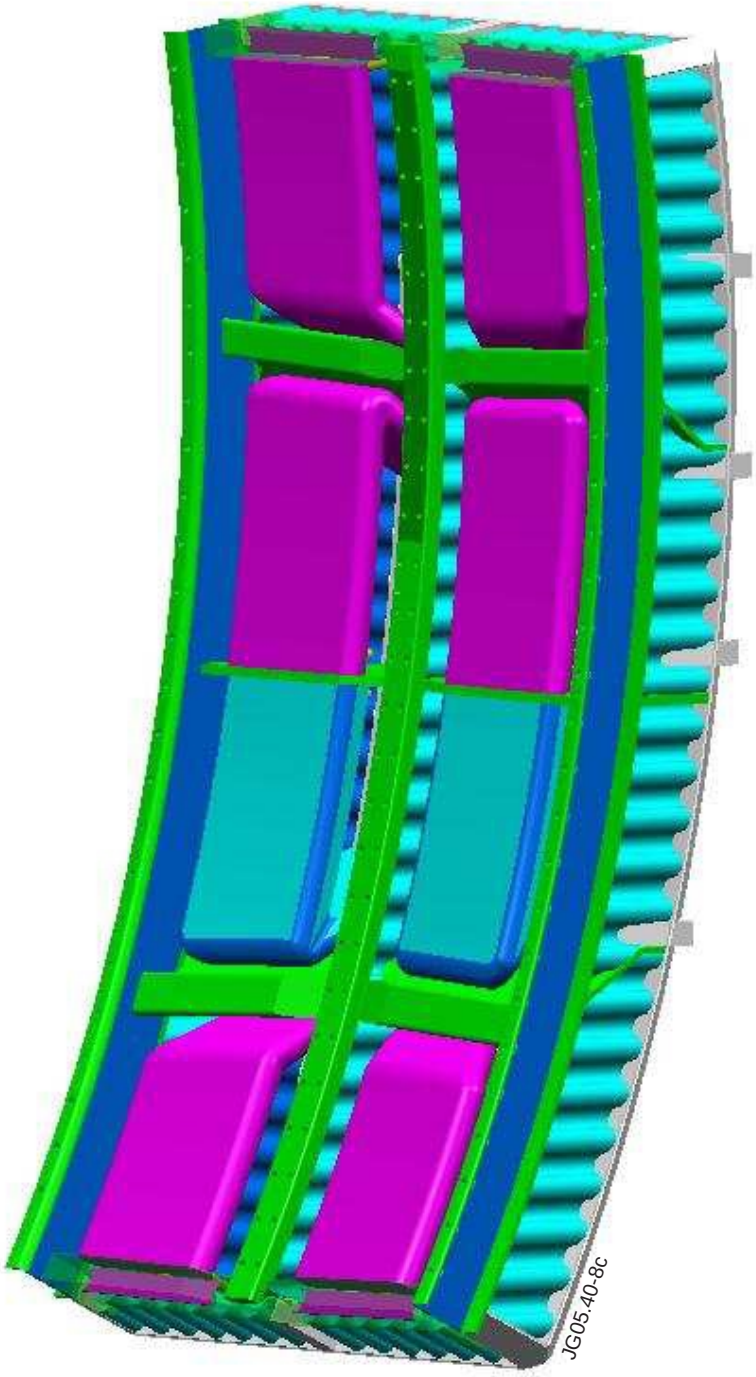

Figure 8: The JET ITER-like ICRF antenna.